



HAL
open science

The interaction dynamics of a negative feedback loop regulates flagellar number in *Salmonella enterica* serovar Typhimurium.

Christine Aldridge, Kritchai Poonchareon, Supreet Saini, Thomas Ewen, Alexandra Solovyova, Christopher V. Rao, Katsumi Imada, Tohru Minamino, Phillip Aldridge

► To cite this version:

Christine Aldridge, Kritchai Poonchareon, Supreet Saini, Thomas Ewen, Alexandra Solovyova, et al.. The interaction dynamics of a negative feedback loop regulates flagellar number in *Salmonella enterica* serovar Typhimurium.. *Molecular Microbiology*, 2010, 78 (6), pp.1416. 10.1111/j.1365-2958.2010.07415.x. hal-00585785

HAL Id: hal-00585785

<https://hal.science/hal-00585785>

Submitted on 14 Apr 2011

HAL is a multi-disciplinary open access archive for the deposit and dissemination of scientific research documents, whether they are published or not. The documents may come from teaching and research institutions in France or abroad, or from public or private research centers.

L'archive ouverte pluridisciplinaire **HAL**, est destinée au dépôt et à la diffusion de documents scientifiques de niveau recherche, publiés ou non, émanant des établissements d'enseignement et de recherche français ou étrangers, des laboratoires publics ou privés.

**The interaction dynamics of a negative feedback loop
regulates flagellar number in *Salmonella enterica* serovar
Typhimurium.**



Journal:	<i>Molecular Microbiology</i>
Manuscript ID:	MMI-2010-10209.R1
Manuscript Type:	Research Article
Date Submitted by the Author:	08-Sep-2010
Complete List of Authors:	<p>Aldridge, Christine; Newcastle University, Centre for Bacterial Cell Biology; Newcastle University, Institute for Cell and Molecular Biosciences</p> <p>Poonchareon, Kritchai; Newcastle University, Centre for Bacterial Cell Biology; Newcastle University, Institute for Cell and Molecular Biosciences</p> <p>Saini, Supreet; University of Illinois at Urbana-Champaign, Department of Chemical and Biomolecular Engineering</p> <p>Ewen, Thomas; Newcastle University, Institute for Cell and Molecular Biosciences</p> <p>Solovyova, Alexandra; Newcastle University, Institute for Cell and Molecular Biosciences</p> <p>Rao, Christopher; University of Illinois, Dept. of Chemical and Biomolecular Engineering</p> <p>Imada, Katsumi; Osaka University, Department of Frontier Biosciences</p> <p>Minamino, Tohru; Osaka University, Graduate School of Frontier Biosciences</p> <p>Aldridge, Phillip; Newcastle University, Centre for Bacterial Cell Biology; Newcastle University, Institute for Cell and Molecular Biosciences</p>
Key Words:	Flagella, Protein:DNA interactions, Gene regulation

The interaction dynamics of a negative feedback loop regulates flagellar number in *Salmonella enterica* serovar Typhimurium.

Christine Aldridge^{1,2}, Kritchai Poonchareon^{1,2}, Supreet Saini³, Thomas Ewen^{1,2}, Alexandra Soloyva², Christopher V. Rao³, Katsumi Imada⁴, Tohru Minamino^{4,5}, and Phillip D. Aldridge^{1,2*}

1: Centre for Bacterial Cell Biology, Medical Sciences New Building, Newcastle University, Richardson Road, Newcastle upon Tyne, United Kingdom, NE2 4AX. 2: Institute for Cell and Molecular Biosciences, Newcastle University, Framlington Place, Newcastle upon Tyne, United Kingdom, NE2 4HH. 3: Department of Chemical and Biomolecular Engineering, University of Illinois at Urbana-Champaign, Urbana, Illinois, United States, 61801. 4: Graduate School of Frontier Biosciences, Osaka University, 1-3 Yamadaoka, Suita, Osaka 565-0871, Japan. 5: PRESTO, JST, 4-1-8 Honcho, Kawaguchi, Saitama 332-0012, Japan.

* Corresponding Author: Email: p.d.aldridge@ncl.ac.uk; Tel: +44-191-208-3218; Fax +44-191-208-3205

Summary

Each *Salmonella enterica* serovar Typhimurium cell produces a discrete number of complete flagella. Flagellar assembly responds to changes in growth rates through FlhD₄C₂ activity. FlhD₄C₂ activity is negatively regulated by the type 3 secretion chaperone FliT. FliT is known to interact with the flagellar filament cap protein FliD as well as components of the flagellar type 3 secretion apparatus. FliD is proposed to act as an anti-regulator, in a manner similar to FlgM inhibition of σ^{28} activity. We have found that efficient growth-dependent regulation of FlhD₄C₂ requires FliT regulation. In turn, FliD regulation of FliT modulates the response. We also show that, unlike other flagellar-specific regulatory circuits, deletion of *fliT* or *fliD* did not lead to an all-or-nothing response in FlhD₄C₂ activity. To investigate why, we characterized the biochemical interactions in the FliT:FliD:FlhD₄C₂ circuit. When FlhD₄C₂ was not bound to DNA, FliT disrupted the FlhD₄C₂ complex. Interestingly, when FlhD₄C₂ was bound to DNA it was insensitive to FliT regulation. This suggests that the FliT circuit regulates FlhD₄C₂ activity by preventing the formation of the FlhD₄C₂:DNA complex. Our data would suggest that this level of endogenous regulation of FlhD₄C₂ activity allows the flagellar system to efficiently respond to external signals.

Introduction

Salmonella enterica serovar Typhimurium utilizes flagella, self-assembled nanomachines anchored in the cell envelope, to swim through liquids and swarm over surfaces. Approximately 60 flagellar genes, organized into 13 operons, are involved in flagellar assembly, motility and chemotaxis. The expression of the flagellar genes follows a strict hierarchy resulting in the subdivision of the flagellar operons into three classes based on the promoters that drive their transcription: P_{class1} , P_{class2} and P_{class3} (Chilcott and Hughes, 2000). There is only one P_{class1} promoter that drives transcription of the genes *flhD* and *flhC*. FlhD and FlhC form a hetero-hexameric complex, FlhD₄C₂, which is the master regulator of the enteric flagellar systems (Wang *et al.*, 2006). FlhD₄C₂ activates transcription itself through a direct interaction with the alpha subunit of RNA polymerase, allowing σ^{70} to activate transcription from FlhD₄C₂ specific promoters (Liu *et al.*, 1995). Previous studies of the FlhD₄C₂ have shown that the DNA binding component is primarily directed through FlhC. FlhD has been proposed to stabilize the FlhD₄C₂:DNA complex (Claret and Hughes, 2000). There are eight FlhD₄C₂-dependent flagellar-specific P_{class2} promoters. One of these promoters drives the transcription of the *fliA* gene, encoding an alternative sigma factor, σ^{28} , required for transcription from the eight P_{class3} promoters (Ohnishi *et al.*, 1990). The gene products of *flhD*, *flhC* and *fliA* are essential for the expression of the flagellar genes.

Along with *fliA*, a further regulatory component transcribed from both P_{class2} and P_{class3} promoters is *flgM*. The gene product of *flgM* is an anti-sigma factor that directly interacts with σ^{28} in the cell, preventing σ^{28} from activating transcription from the P_{class3} promoters during HBB assembly (Gillen and Hughes, 1991a; Gillen and Hughes, 1991b). Upon HBB completion P_{class3} activation is coupled to flagellar assembly through the

physical secretion of FlgM via the flagellum, thus freeing σ^{28} to activate transcription from P_{class3} promoters (Hughes *et al.*, 1993; Kutsukake and Iino, 1994).

The coupling of assembly and gene expression suggests that some gene products are only expressed at a given stage of the assembly pathway. However, one limitation of this model is that it only considers a single flagellum. *S. enterica* does not produce a single flagellum per cell. Rather, it produces many, approximately four to eight per cell (Iino, 1974). Thus, in a growing cell with more than one flagellum, all components required to assemble a complete flagellum are in theory present. Therefore, the flagellar system likely requires additional levels of control in the presence of growing or assembled flagella that allow it to coordinate and adjust flagellar gene expression accordingly. Specifically, the presence of an upper limit in flagella number suggests that a negative feedback loop, sensitive to the number of flagella present, exists to modulate the activity of the regulators FlhD₄C₂ and σ^{28} .

For σ^{28} :FlgM, the physical secretion of FlgM itself through completed HBB structures provides a given level of control for σ^{28} . We have recently shown that changing the rate of FlgM secretion modulates σ^{28} activity (Brown *et al.*, 2008). Ideally, a level of negative feedback similar to the σ^{28} :FlgM circuit would regulate the activity of the master regulator FlhD₄C₂ in response to flagellar assembly. As FlhD₄C₂ is at the top of the transcriptional hierarchy, any changes in its activity will have the net effect of reducing both P_{class2} activity and σ^{28} -dependent activation of P_{class3} . Other than FlgM and σ^{28} , there are two regulatory proteins that modulate flagellar gene transcription: FliT and FliZ (Kutsukake *et al.*, 1999; Saini *et al.*, 2008; Yamamoto and Kutsukake, 2006). The necessary negative feedback required to regulate FlhD₄C₂ activity to secretion is the anti-FlhD₄C₂ factor, FliT (Yamamoto and Kutsukake, 2006). FliT is known to inhibit FlhD₄C₂-binding to DNA

through its direct interaction with FlhC (Yamamoto and Kutsukake, 2006), while it also interacts with the filament-capping protein FliD and two soluble proteins, FliI and FliJ, of the flagellar T3S apparatus (Evans *et al.*, 2006; Fraser *et al.*, 1999; Imada *et al.*, 2010). FliJ enhances FliT/FliD interactions with the C-terminal cytoplasmic domain of FlhA, a key protein of the flagellar-specific type III secretion apparatus (Bange *et al.*; Saijo-Hamano *et al.*). The interactions of FliT with FliD, FlhA and FliJ are thought to facilitate the secretion of FliD upon completion of the HBB. With respect to its interaction with FlhC, FliT has been defined as an anti-FlhD₄C₂ factor and FliD an anti-anti-FlhD₄C₂ factor (Yamamoto and Kutsukake, 2006). In this regulatory circuit, FlhD₄C₂ would regulate flagellar assembly in response to the rate of FliD secretion.

FliT consists of four α -helices (α 1, α 2, α 3, and α 4) (Imada *et al.*, 2010). A truncation of the C-terminal α 4-helix, leading to FliT94, increases the binding affinity for the FlhD₄C₂ complex, suggesting that α 4 plays an autoregulatory role in modulating FliT activity. A surface exposed residue Lys-79 in α 3 is critical for the interaction with FliD. The α 4 helix binds to the hydrophobic cleft formed by α 2 and α 3. As a truncation of α 4 does not affect the interaction with FliD or FlhD₄C₂ *per se*, it is proposed that the interaction between α 4 and the hydrophobic cleft modulates the binding affinity for the FlhD₄C₂ complex (Imada *et al.*, 2010).

In this work, we investigate the role of FliT regulation of FlhD₄C₂ during continual flagellar assembly. We show that FliT regulation of FlhD₄C₂ activity allows the system to efficiently respond to bacterial growth rates. In addition, unlike the all-or-nothing response observed with respect to the deletion of *fliA* (σ^{28}) or *flgM*, genetic analysis of the FliT circuit suggests FliT tunes the activity of the FlhD₄C₂, but never switches it off. To investigate the mechanism behind this behavior, we performed a biochemical characterization of the

FliT:FliD:FliH₄C₂ circuit. Using this approach, we show that FliT regulates FliH₄C₂-dependent activation of P_{class2} by disrupting the FliH₄C₂ complex. However, FliT-dependent inhibition is unable to disrupt the FliH₄C₂-DNA complex. Based on our results, we propose the model that FliT regulation of FliH₄C₂ allows the flagellar system to respond efficiently to external regulatory inputs directed through changes in FliH₄C₂ activity.

For Peer Review

Results

The assembly of flagella in *S. enterica* responds to changes in growth rates.

Recently a two-fold change in *flhDC* gene expression was shown to increase flagellar numbers by two-fold (Erhardt and Hughes). This study used, in part, a chromosomally encoded, functional FliM-GFP fusion to numerate flagella by the number of HBB per cell (Aldridge *et al.*, 2006a). A significant number of studies over the past 5 decades monitor *S. enterica* flagellar assembly in LB. We asked if the growth conditions were changed, would a similar flagella distribution or a growth dependent phenotype be observed. Using the FliM-GFP construct we counted the number of HBB per cell of *S. enterica* grown in four conditions. We used a minimal medium base (Minimal E plus 0.2% Glucose) containing increasing amounts of Yeast Extract (YE) (0.04 g/L, 0.2 g/L, 1 g/L and 3 g/L). Yeast extract was chosen, as it could increase growth rates to that equivalent of LB (3 g/L YE (data not shown)). Growth was performed at 30°C for consistency with previous experiments performed (Brown *et al.*, 2008). The rationale of adding rich nutrients to a base medium was similar to seminal growth experiments performed by Schaechter *et al.*, to observe changes in growth mass in *S. enterica* at different growth rates (Schaechter *et al.*, 1958).

Flagellar numbers were counted at late exponential phase of standard shaken cultures prior to the transition into stationary phase (Figure 1A, Figure S1 and Table 1). This time point is suggested to coincide with maximal flagellar gene expression (Pruss and Matsumura, 1996; Pruss and Matsumura, 1997). We observed an unexpected growth dependent phenotype that went against our perception of flagella utilisation. In our nutrient limiting conditions (0.04 g/L YE) we observed a significant reduction in flagellar numbers compared to 3 g/L YE. Changing carbon source or using a defined amino acid mix did not

alter this response (data not shown). On average, growth in 0.04 g/L YE produced 0.3 flagella/cell, while 3 g/L YE produce 3.74 flagella/cell (Table 1). No cells were observed for 0.04 g/L YE with more than 2 foci (Figure 1A). In contrast to growth in 0.04 g/L that exhibited an exponential distribution of flagellar numbers, 3 g/L YE growth produced a Gaussian (or normal) distribution of flagellar numbers. For the 3 g/L YE population, 90% of cells observed possessed one or more foci (Table 1). This suggests that only when nutrients are perceived will flagellar numbers increase, dependent on nutrient availability, to achieve optimal swimming behavior and therefore chemotaxis. These observations are consistent with previous reports on the influence of media composition on the flagellation of *E. coli* (Adler and Templeton, 1967).

FliT regulation is required to allow the system to respond accurately to external signals

The response of the *S. enterica* flagellar system to growth conditions suggests the system is flexible enough to respond to external cues, even though motility is defined as a robust phenotype (Barkai and Leibler, 1997). The majority of external signals are transduced into the flagellar system through changes in *flhDC* expression or FlhD₄C₂ stability, observable as a change in FlhD₄C₂ activity (Soutourina and Bertin, 2003). Yamamoto and Kutsukake (2006) have shown that FlhD₄C₂ activity is negatively regulated via a direct interaction with FliT. This suggests that FlhD₄C₂ activity is regulated by internal signals from the flagellar system. In their work, it was proposed that FliD regulates the ability of FliT to inhibit FlhD₄C₂ activity (Yamamoto and Kutsukake, 2006). Therefore, FliT regulation of FlhD₄C₂ activity sensitises the system to flagellar assembly via FliD secretion rates (Brown *et al.*, 2008). As a growth dependent phenotype for flagella numbers was observed, we asked which level of regulation was dominant, the external regulation of FlhD₄C₂ or the

endogenous regulation through FliT. We therefore compared FliM-GFP foci numbers in our growth conditions for $\Delta fliT$ and $\Delta fliD$ mutants to wild type (Figure 1B and C).

We observed a significant increase in flagellar numbers at all growth rates for the $\Delta fliT$ mutant compared to wild type (Figure 1B and Figure S1). The percentage of cells with foci also significantly increased for the $\Delta fliT$ mutant compared to wild type. Grown in 0.04 g/L YE 60% of cells from the $\Delta fliT$ mutant population contained FliM-GFP foci as compared to 24% in wild type. The average number of FliM-GFP foci in the $\Delta fliT$ mutant also increased in all conditions (Table 1). Consistently, a reciprocal drop in flagellar numbers was observed for the $\Delta fliD$ mutant (Figure 1C, Figure S1, and Table 1). Even for 3g/L YE the 54% of foci containing cells of the $\Delta fliD$ mutant had only one or two foci (16/50 cells) with only a small proportion having 3 foci (4 cells), 4 foci (3 cells), 5 foci (2 cells) or 6 foci (2 cells) (Figure 1C). Importantly, the $\Delta fliT$ and $\Delta fliD$ phenotypes were observed at all growth rates, suggesting that the level of regulation exerted through FliT on FlhD₄C₂ is independent of growth. Furthermore the data suggests that for the system to respond to external cues efficiently, endogenous regulation of FlhD₄C₂ by FliT is required.

Overexpression of *fliT* does not halt flagellar gene expression completely.

Consistent with the flagellar numbers of the $\Delta fliT$ and $\Delta fliD$ mutants, plasmid-based expression of *fliT* or *fliD* resulted in the expected change. An increase of full-length *fliT* concentration by approximately 4 fold (data not shown) was unable to completely inhibit movement as assayed using motility agar plates (Figure 2A). This level of increased *fliT* expression resulted in only 2 % of cells possessing one FliM-GFP foci in comparison to 90 % in wild type. The recent description of the FliT structure suggested that a C-terminal α -helix modulates FliT activity (Imada *et al.*, 2010). Deletion of this α -helix, producing the

variant *fliT94*, resulted in a further reduction in motility on motility agar after 8 hours incubation when *fliT94* was expressed from a high copy number plasmid (pSE-*fliT94*) or as a GST fusion protein (pGST-*fliT94* (pMMT002) - Figure 2A) (Imada *et al.*, 2010). In comparison, overexpression of either *flgM* or *fliA* from pSE380 did not reduce motility in soft agar plates significantly (Figure 2A). This suggests that the σ^{28} :FlgM and FliT regulatory circuits play distinct roles in regulating flagellar assembly, albeit that they are interlinked by σ^{28} -dependent transcription of the *fliDST* operon.

We have recently established a flagellar gene expression assay that monitors flagellar gene expression through a Fla⁻ to Fla⁺ transition (Brown *et al.*, 2008). The motility phenotypes of plasmid-based expression of *fliT* and *fliT94* suggest that a basal level of flagellar gene expression is still present. To confirm this, flagellar gene expression dynamics were measured for plasmid-based *fliT* or *fliT94* expression from pSE380 (Figure 2B). As compared to wild type, plasmid-based expression of *fliT* and *fliT94* resulted in a significant delay in activation of P_{class2} and P_{class3} promoters. However, the flagellar transcriptional hierarchy was still evident in all strains (Figure 2B). When expressing *fliT*, P_{flgA} activity peaked at 1672 RLU at 91 minutes, a 4.9 fold reduction compared to its vector control that peaked at 8219 at 119 minutes. For *fliT94* P_{flgA} activity reached a maximum activity of 1067 RLU at 98 minutes, a 7.7 fold reduction in activity. For the P_{class3} promoter P_{fliC}, *fliT* and *fliT94* expression resulted in maximum activity of 130 and 118 RLU respectively compared to 15339 RLU for the vector control. These observations are consistent with the proposed function of $\alpha 4$ modulating FliT activity by binding into a cleft formed by helices $\alpha 2$ and $\alpha 3$. Importantly, both constructs were unable to completely inhibit flagellar gene expression. Instead, flagellar gene expression is significantly reduced to a basal level that can still sustain some motility. Therefore, this suggests that for the

observed phenotypes, some aspect of the FliT:FlhD₄C₂ regulatory circuit prevents FliT completely inhibiting FlhD₄C₂ from activating flagellar gene expression.

FliT disrupts the free FlhD₄C₂ complex

The *in vivo* data on FliT regulation suggests that even in excess, FliT is unable to completely inhibit FlhD₄C₂. Instead, the data suggests that FliT acts to significantly reduce FlhD₄C₂ activity. However, the *in vivo* data does not offer an explanation to how this level of regulation by FliT is achieved or why it exists. We therefore investigated the biochemical characteristics of the FliT regulatory circuit *in vitro* to determine if the nature of the interactions between FliT, FliD, FlhD₄C₂ and the FlhD₄C₂ DNA binding site could aid our understanding of FliT regulation *in vivo*.

Yamamoto and Kutsukake (2006) were able to show that FliT interacts with FlhC of the FlhD₄C₂ complex. All *in vitro* analysis in this work focussed on FliT regulation of the FlhD₄C₂ complex rather than FlhC itself. The rationale for this approach argued that to understand the *in vivo* data, how the FlhD₄C₂ complex behaves in the presence of FliT rather than FlhC alone was important. We began by asking whether we could isolate an FlhD₄C₂:FliT complex. FlhD₄C₂ and FliT were purified separately, mixed at different molar ratios and subjected to gel filtration. No high molecular weight species characteristic of a stable FliT:FlhD₄C₂ complex was observed (data not shown). The analyses of the FliT:FlhD₄C₂ interaction using surface plasma resonance (SPR) and isothermal calorimetry were unable to add any value to understanding the gel filtration data. We therefore utilised analytical ultra-centrifugation (AUC) to characterise the FliT:FlhD₄C₂ interaction further (Figure 3).

FliT exists in equilibrium between its monomeric and dimeric form in solution, as judged by sedimentation equilibrium AUC measurements (Imada *et al.*, 2010). Analysis of FlhD₄C₂, by sedimentation velocity AUC, produced a single protein species with a mass of 94.9 kDa. This is in good agreement with the theoretical mass of the FlhD₄C₂ complex (96.7 kDa) (Wang *et al.*, 2006). Addition of FliT to FlhD₄C₂ at a 1:1 molar ratio using 8 μM FlhD₄C₂ did not produce a high molecular weight species larger than 94.9 kDa. Instead the FlhD₄C₂ peak was reduced in size and a long shoulder that tapered towards the left of the FlhD₄C₂ peak appeared. Higher ratios of FliT:FlhD₄C₂ were then analysed and resulted in the shoulder becoming a defined peak with a predicted mass of 61-63 kDa. According to the size of this new protein species we assume that it could either be the dissociated FlhD₄ tetramer or a FliT:FlhC₂ complex. This data suggests that on interaction of FliT with FlhD₄C₂, the net result is the disassociation of the FlhD₄C₂ complex through the interaction of FliT with FlhC. This is in agreement with a previous report that the amount of FlhD co-eluted with GST-FliT94 from a GST column is much lower than that of FlhC (Imada *et al.*, 2010).

Inhibition of FlhD₄C₂:DNA complex formation requires excess FliT

Within the FliT regulatory circuit, the key interaction is FlhD₄C₂-binding to its DNA binding site. Based on our AUC results, we speculated that excess amounts of FliT would provide increased inhibition of FlhD₄C₂:DNA binding. To test our hypothesis, we chose a SPR approach. We immobilized 350-400 RU of double stranded 80-mers, biotinylated on one strand, to a streptavidin sensor chip containing the FlhD₄C₂ DNA binding site from *flgB* (*P_{flgB}*) and *flhB* (*P_{flhB}*) and an intergenic region of *fliC* coding sequence as a control DNA. Consecutive injections of FlhD₄C₂ in a dilution series to *P_{flgB}* DNA exhibited a concentration dependent response (Figure 4A). Addition of FliT in a 1:1 ratio with FlhD₄C₂ prior to

injection resulted in a significant reduction in FlhD₄C₂:DNA interaction but did not completely inhibit it (Figure 4A). Analysis of the data showed that V_{max} for FlhD₄C₂ alone to be 3933 compared to 560 for FlhD₄C₂ and FliT (Table S2). Binding to P_{flhB} and *fliC* DNA (data not shown) showed consistency with previous studies on the FlhD₄C₂:DNA interaction. Stafford *et al.* showed that FlhD₄C₂ could bind to DNA without a defined FlhD₄C₂ binding site (Stafford *et al.*, 2005; Wang *et al.*, 2006). Therefore, the observation that FlhD₄C₂ bound to a coding region of *fliC* is not that surprising.

Our AUC data suggested that increasing molar ratios of FliT:FlhD₄C₂ would significantly disrupt the FlhD₄C₂ complex. Using our SPR assay the ability of increasing FlhD₄C₂:FliT ratios to inhibit FlhD₄C₂ to bind its DNA binding site were tested. Increasing amounts of FliT were added to 100 nM FlhD₄C₂ giving the ratios of 1:1, 1:1.5, 1:2.5 and 1:4 prior to injection over P_{flgB} (Figure 4B). Increasing amounts of FliT significantly reduced the ability of FlhD₄C₂ to bind to its binding site (Table S2). Molar ratios higher than 1:4 gave similar results (data not shown) suggesting that the maximal level of inhibition in our assays of the FlhD₄C₂ to DNA interaction is a ratio of approximately 1:4.

A FlhD₄C₂:DNA complex is resistant to FliT regulation

The above observations from our AUC and initial SPR analysis are sufficient to explain the observed phenotypes of the $\Delta fliT$ and $\Delta fliD$ mutants and *fliT* overexpression with respect to FliM-GFP foci. Our data suggests that to completely inhibit FlhD₄C₂ a high ratio of FliT to FlhD₄C₂ is required. Previous studies characterising the FlhD₄C₂:DNA interaction have established that the FlhD₄C₂:DNA complex is very stable with a half-life of approximately 40 minutes (Claret and Hughes, 2000). Thus, irrespective of the level of free FliT, its regulation of FlhD₄C₂ will potentially encounter FlhD₄C₂ bound to DNA. Therefore we

asked what effect would FliT have upon an FlhD₄C₂:DNA complex using our SPR assay (Figure 5). The injection of PBS running buffer did not show any effect, as expected. Unexpectedly, FliT would not disrupt the already existing FlhD₄C₂:DNA complex (Figure 5A - addition of a 100 nM solution of FliT to bound FlhD₄C₂ complexes is shown). In these assays a constant concentration of 100 nM FlhD₄C₂ was first bound to the immobilised DNA. Even a 100-fold excess of FliT (10 μM) could not disrupt the FlhD₄C₂:DNA complex (data not shown). In contrast and as a control to show that FlhD₄C₂ was bound and could be disassociated, injecting 100 nM free P_{flgB} DNA resulted in disassociation of the FlhD₄C₂:DNA complex from all 3 DNA species tested (Figure 5B). Importantly, this control also showed that the interaction dynamics of FlhD₄C₂ with the three DNA species behaved in agreement with a previous work (Stafford *et al.*, 2005). These results, therefore, suggest that FliT can prevent FlhD₄C₂ from binding DNA but if FlhD₄C₂ is already bound to DNA, FlhD₄C₂ is resistant to FliT regulation.

FliD acts as an anti-anti-FlhD₄C₂ factor

The phenotype of a $\Delta fliD$ mutant with respect to changes in flagellar gene expression and that FliD directly interacts with FliT led Yamamoto and Kutsukake (2006) to propose that FliD acts as an anti-anti-FlhD₄C₂ factor. However, this hypothesis has not been experimentally explored. We therefore used the SPR-based assay of FlhD₄C₂ binding DNA to observe what effect FliD would have upon FliT inhibition of FlhD₄C₂.

As FliD:FliT interact in a 1:1 molar ratio, a 1:1:1 ratio of FliD:FliT:FlhD₄C₂ was assayed. Addition of FliD to FlhD₄C₂, in the absence of FliT, did not alter the ability of FlhD₄C₂ to bind DNA (Figure 6). This was in agreement with gel filtration and bacterial two-hybrid analysis that did not identify a FliD:FlhD₄C₂ interaction (data not shown). In

contrast, a mix of FliD, FliT and FlhD₄C₂ did alter the ability of FliT to inhibit FlhD₄C₂ from binding DNA (Figure 6). A similar response to the addition of FliD to a 1:1 mix of FliT94:FlhD₄C₂ was also observed (Figure S2). Therefore we can confirm Yamamoto and Kutsukake's proposal that FliD does act in an anti-anti-FlhD₄C₂ manner. Interestingly, a complete inhibition of FliT regulation was not observed.

The FliD/FlhD₄C₂ binding sites on FliT overlap

The data above suggests that FliD interaction with FliT when all proteins are at a 1:1:1 ratio is not sufficient to completely inhibit the regulation of FlhD₄C₂ by FliT. One explanation for this is that the binding sites for FliD and FlhD₄C₂ are on distinct surfaces of FliT. As a result even in the presence of FliD, FliT could disrupt the FlhD₄C₂ complex. An alternative explanation is that the sites of interaction overlap and the observed response is due to FliD/FlhD₄C₂ competition for FliT. To distinguish between these two models, a genetic analysis of *fliT* was performed. Our intent was to determine if *fliT* point mutations would exist that could bind FliD but not interact with FlhD₄C₂ and vice versa. The P_{class1} *flhDC* promoter is negatively autoregulated by FlhD₄C₂ (Figure 7). Deletion of *fliT* although observed to have increased P_{class2} activity, exhibits reduced P_{class1} activity (Figure 7). This suggests that FliT regulation effects not only P_{class2} activity but also FlhD₄C₂ levels through regulation of the autoregulatory control of the P_{class1} promoter region by FlhD₄C₂. Our screen used the drop in P_{class1} activity associated with loss of FliT regulation to isolate *fliT* mutations exhibiting reduced activity against FlhD₄C₂. Mutations in *fliT* were isolated using random PCR mutagenesis (Aldridge *et al.*, 2006b). From 2000 colonies, 17 colonies with reduced P_{class1} activity were isolated randomly and sequenced. From these 9 had single point mutations, 3 had two point mutations, 2 had triple mutations, one had a C-terminal extension of 25 amino acids due to the mutation of the stop codon and one did not contain

any mutation in the coding sequence of *fliT* (data not shown). Using the recently described structure of FliT the single point mutations were found to all cluster in $\alpha 1$ or $\alpha 3$. Interestingly, one mutation N74D was at the same residue as had been identified to show weaker FliD interaction (Imada *et al.*, 2010). This suggests that the FliD and FlhD₄C₂ binding sites on FliT may in fact overlap.

To further investigate whether the FliD/FlhD₄C₂ binding sites on FliT overlap, we assayed alanine substitution mutants in the C-terminal portion of $\alpha 3$ in motility assays, an FlhC pull-down assay (Imada *et al.*, 2010) and the SPR-based assay. Motility assays of these mutations introduced into *fliT94* showed that five exhibited a strong reduction in the ability of *fliT94* to inhibit motility: I68A, N74A, E75A, K79A and L82A (Figure 8A). Consistently, in a pull-down assay one of these mutations (E75A) showed a significant drop in its ability to interact with FlhC compared to those that showed a similar phenotype to wild type *fliT94* (Figure 8B).

Four substitutions showing motility were also assayed for their ability to inhibit the FlhD₄C₂:DNA interaction. In agreement with the motility and pull-down assays FliT94(E75A) exhibited the weakest inhibition of the DNA interaction (Figure 8C and Table S2). In contrast, the substitutions K79A and L82A behaved in a similar fashion showing inhibition at ratios greater than 1:2 of FlhD₄C₂:FliT94, while N74A exhibited a slight drop in inhibition at all concentrations. Importantly, all alanine substitutions still retained the ability to bind to FlhC to some extent and therefore inhibited wild-type motility (Figure 8). Therefore, these mutants strongly suggest that the FliD/FlhD₄C₂ interface on FliT somehow overlap and the observed response in the SPR analysis is the result of competition for FliT.

Discussion

A key factor often overlooked with respect to flagellar assembly is how the cell coordinates the synthesis of multiple flagella during bacterial growth. Here we have presented evidence suggesting that enteric bacteria are able to sense the extent of their flagellation via an endogenous regulatory circuit that modulates the activity of FlhD₄C₂. Furthermore this internal regulation is key to allow the system to respond accurately to extracellular environmental, internal metabolic or growth dependent signals.

Two key observations from this study showed that i) loss of FlhD₄C₂ regulation by FliT disrupted an efficient response to changes in growth conditions and ii) if bound to DNA, FlhD₄C₂ was insensitive to FliT regulation. Consistent with both observations was the finding that deleting *fliD* or expressing full length or a truncated *fliT* variant from a plasmid was unable to completely inhibit FlhD₄C₂ activity in any growth condition. That when bound to DNA, FlhD₄C₂ was insensitive to FliT regulation is an intriguing twist to an already complex regulatory network that couples flagellar gene expression to the assembly pathway.

Hughes and co-workers predicted that FlhC was the major DNA binding component of the FlhD₄C₂ complex (Claret and Hughes, 2000). Yamamoto and Kutsukake (2006) when describing the FliT:FlhD₄C₂ interaction were able to show that FliT was interacting with FlhC. Our data are in agreement with these observations. The resistance of the FlhD₄C₂:DNA complex to FliT suggests that the FliT binding site on FlhC overlaps the FlhC DNA binding domain. This is different than the model presented by Wang *et al.*, (2006) when FlhD₄C₂ was crystallised. Wang *et al.*, (2006) proposed a configuration that shows FlhD being the major DNA binding component. However, when discussing this model, they

conceded that the data available were insufficient to rule out other plausibility's, such as FlhC making the majority of the DNA:protein contacts (Wang *et al.*, 2006). Our data, with that of the co-workers of Hughes and Kutsukake suggests that the proposed alternative is more feasible but still requires direct biochemical or structural evidence to confirm the correct orientation.

Our genetic analysis of the FliT:FlhD₄C₂ interaction suggests that it is not only the interaction sites of FliT and DNA on FlhC that overlap. Mutations in FliT itself, previously shown to reduce FliD interaction, were also found to have reduced activity in inhibiting FlhD₄C₂ (Imada *et al.*, 2010). A conclusion based on the analysis of alanine substitutions in the truncated variant FliT94. The genetic analysis, in conjunction with our biochemical analysis, suggests that a key factor in the way that FliT regulates FlhD₄C₂ is the extent of competition between all components. As a result this circuit is sensitive to the availability of FliT to bind FliD, FliT to bind FlhC and the availability of FlhD₄C₂ to bind DNA. A swing in the balance between these three reactions will alter the level of FlhD₄C₂ output in terms of transcription activation.

In agreement with previous data we have shown that FlhD₄C₂ can bind DNA un-specifically (Stafford *et al.*, 2005). The mode of binding may be different, as seen during the competition assays using unbiotinylated P_{flgB} DNA to disassociate the FlhD₄C₂:DNA complexes (Figure 5B). The ability of FlhD₄C₂ to bind DNA even without a defined binding site could potentially have an impact of FliT regulation as it means FlhD₄C₂ does not only have to bind to its specific sites to become resistant to FliT.

What is the advantage of FlhD₄C₂ being regulated by FliT only when not bound to DNA? A recent study using SPR, which our assays were based on, showed that the

RelBE system behaves somewhat different to FlhD₄C₂ regulation by FliT. The RelBE system is a toxin-antitoxin locus in which the toxin component can cleave mRNA associated with ribosomes but also autoregulates the transcription of the *relBE* locus (Overgaard *et al.*, 2008). If RelE interacts with a RelB:DNA complex the result is disassociation of the proteins from the DNA (Overgaard *et al.*, 2008). The flagellar and RelBE systems are very different with respect to their regulation. For the flagellar system there is an advantage for a given basal level of activity to exist even when *flhDC* expression is under significant negative influence from the long list of regulators that can influence its expression (Soutourina and Bertin, 2003). Both a P_{class2} and a P_{class3} promoter drive the transcription of *fliT*. Thus, even at low levels of *flhDC* expression some FliT can be made, even if no complete HBBs are present. The apparent competition between all components that our data suggests, predicts that even during HBB assembly, when FliD is not being secreted, a given level of FliT would be available to interact with free FlhD₄C₂. Note also that activation of FlgM secretion allows σ^{28} to increase transcription of *fliT*. Therefore once one structure is complete the level of free FliT will increase due to changes in FliD and FlgM levels as a result of secretion. We propose the working model that under growth conditions that exhibit significant inhibition of *flhDC* expression, FliT regulation will control the extent of flagellation by further inhibiting any free FlhD₄C₂ found in the cell. However, if the FlhD₄C₂:DNA interaction occurs first then bound FlhD₄C₂ will be insensitive to FliT regulation.

Our data suggests that under certain environmental conditions a basal level of FlhD₄C₂ activity is maintained via a balance between external regulation of *flhDC* expression and internal regulation through, for example, FliT inhibition of FlhD₄C₂. The result is that a small proportion of cells amongst the population will possess a low number of flagella. It is then the subpopulation of flagellated cells that are able to begin to move

out of the current location to seek more preferential growth conditions. Adler and Templeton (1967) drew similar conclusions from their work to gain maximum motility of *E. coli* in a defined chemical medium. Interestingly, how efficient chemotaxis would be in *E. coli* or *S. enterica* cells possessing low flagella numbers has not been explored in detail and in the light of this work would be an interesting line of investigation (Darnton *et al.*, 2007; Turner *et al.*, 2000).

Thus, in conclusion we have shown that the enteric flagellar system requires a given level of endogenous negative feedback regulation to respond to external signals. For enteric bacteria this regulation is via the negative regulation of FlhD₄C₂ activity by FliT. We further conclude that FliT is unable to completely inhibit FlhD₄C₂ from activating flagellar gene expression, thus preparing the population to respond, with respect to the flagellar system, accordingly to external signals. What is now of interest is to begin to question how non-FlhD₄C₂ dependent systems control the same response.

Materials and Methods

Bacterial Strains, Plasmids and Cultivation

Strains and Plasmids used during this study are described in Table 2. Media used in this study included LB broth and Minimal E (Davis *et al.*, 1980; Vogel and Bonner, 1956). All plates contained 1.5% agar. Motility assays were performed using semi-solid motility agar containing 0.3% difco agar. Cultures were grown at either 37°C or 30°C with constant shaking at 180 rpm. Antibiotic concentrations have been described previously (Bonifield *et al.*, 2000). For the growth condition experiment Minimal E base salts were supplemented with 0.2% glucose and the stated concentration of Yeast extract from a stock solution of 25 g/L. For purification of FliT, FliD and FliH₄C₂ LB cultures were grown to an OD₆₀₀ nm between 0.4 and 0.6 at 37°C. Induction of expression for 3 to 5 hours was achieved using a final concentration of 1 mM IPTG with incubation at 30°C. Cell pellets were harvested and stored at -80°C until needed.

DNA Manipulation

Throughout this study standard cloning and DNA manipulation techniques have been used. All plasmids were sequenced prior to use. Primer sequences used for constructs are available on request. A modified version of pET28a-mod was used in this study that reduced the size of the his-tag fused to FliT or FliD with a region of the multiple cloning site deleted (Table 2). For the purification of FliH₄C₂ the entire *flhDC* operon was subcloned into pET28a-mod. On induction this produced a complex that was his-FliH₄C₂. All protein identities were also confirmed by MALDI-TOF analysis using an in-house facility at Newcastle (PINNACLE).

Random mutagenesis of *fliT* was performed using the natural error rate of Taq DNA polymerase. A PCR reaction generated using Taq DNA polymerase was recombined onto the chromosome of strain TPA993 selecting on Tetracycline-sensitive (Tet^S) plates (Aldridge *et al.*, 2006b). After selection, crossing once more on to Tet^S plates was used to isolate 2000 colonies. A pool of the 2000 colonies was then transduced with plasmid pRG38 ($P_{fihDC}::luxABCDE$) to screen for potential *fliT* mutants. To isolate colonies exhibiting reduced light production, images of the transduction plates were made using the chemiluminescent settings of an intelligent light box. Seventeen colonies were taken at random and purified to isolate phage free colonies before light production was confirmed using liquid cultures assayed in a BMG Fluostar microplate reader. The *fliT*-coding region was then sequenced from PCR products. Deletion of *fliD* in TPA2421 used previously described recombineering protocols (Aldridge *et al.*, 2003; Datsenko and Wanner, 2000).

Epifluorescent Microscopy

To visualise FliM-GFP, cultures were grown as described above. At appropriate time points or OD600 nm values, one microlitre of culture was spotted onto a 1% agarose pad containing 1 x E-salts but no glucose in a Gene frame (AB gene). The agarose pad was sealed with a coverslip, a procedure sufficient to immobilize the motile bacteria. Images were acquired on a Zeiss Axiovert 200M system (Murray and Errington, 2008). An exposure time for all GFP images of 1.5 seconds was used and 100 milliseconds for a phase contrast image. Images were captured through METAMORPH (version V.6.2r6) and then processed using ImageJ (NIH).

To count FliM-GFP foci all cells were counted using the dot function of ImageJ. From the counted cells a random number generator (www.randomizer.org) was used to identify 50 cells from each time point and strain. Using a stacked RGB composite image of

the GFP and phase contrast images, the FliM-GFP foci were then counted manually in the identified cells. Histograms of the number distributions and statistical analysis were performed using Excel (Microsoft).

Protein Purification

All protein isolations were done using an Akta *Prime Plus* (GE Healthcare). Purification of FliT and FliD was performed using standard purification protocols. Briefly, cell pellets of induced cultures were resuspended in His-loading buffer: 50 mM HEPES, 150 mM NaCl, 20 mM Imidazole, pH 7.5 and sonicated for 5 min on ice. To remove all cell debris the sample was centrifuged at 31,500 x g for 30 min at 4°C prior to injection over a pre-equilibrated 5 ml his-trap column (GE Healthcare). Proteins were eluted using an 80% Imidazole gradient over 50 ml of His-elute buffer: 50 mM HEPES, 150 mM NaCl, 1 M Imidazole, pH 7.5.

FliD₄C₂ purification was performed using a modified method described by Wang *et al.*, (2006). Plasmid pPA158 was freshly transformed into BL21 and induced cell pellets isolated from up to 6 litres of culture and resuspended in Buffer A: 20 mM Tris, pH 7.9. The cell suspension was sonicated for 5 min, centrifuged for 30 min at 31,500 x g at 4°C and injected over a 5 ml Heparin column (GE Healthcare). After injection, the column was washed with a 20% solution of Buffer B: 20 mM Tris, 1 M NaCl, pH 7.9. After the baseline reached a pre-loading level, elution of the FliD₄C₂ complex was achieved using a gradient of Buffer B up to 100% applied over 60 minutes. All protein fractions were checked by SDS page on 16.5% Tricine gels.

After purification FliT, FliD and FliD₄C₂ proteins were concentrated using VIVAspin columns (10 kDa cutoff) and subjected to gel filtration using a S200 column (GE

Healthcare). The gel filtration buffer used was 20 mM Tris, 300 mM NaCl, 1 mM DTT, pH 7.9. Pull down assays by GST affinity chromatography have been previously described (Imada *et al.*, 2010).

Surface Plasma Resonance

The majority of SPR experiments were performed using the BIAcore 2000. Experiments using FliT94 were performed on a Bio-Rad Proteon XPR36. DNA-protein interaction experiments were done using a streptavidin (SA) or neutravidin coated sensor chips (GE Healthcare and Bio-Rad). The running buffer for all experiments was phosphate buffered saline (PBS). For the DNA-protein experiments using the BIAcore 2000 365 resonance units (RU) of DNA were immobilized on the SA sensor chip, while for the XPR36 100 RU were immobilized. Prior to immobilization, 3 consecutive injections over all flow cells for 60 seconds at a flow rate of 10 μ l / min with 1M NaCl then 0.05 M NaOH were performed to ensure no contamination of unspecific bound compounds. An empty flowcell was always used as a negative control for background subtraction and therefore had no DNA or protein bound to it. The DNA used was an 80 bp double-stranded oligonucleotide, with a 5'biotinylated forward strand of the *flgB* and *flhB* binding sites of FlhD₄C₂ (Table 3) (Stafford *et al.*, 2005). Also as a negative control we used an intergenic region of *fliC* (Table 3). Annealing of the DNA was performed using a Biometra T3000 Thermocycler: 94 °C for 2 min then ramp cooled to 25 °C over 45 min then kept at 4 °C until use. Annealing of samples was confirmed by native gel electrophoresis on 10% native gels. For all experiments FlhD₄C₂ protein was applied for 60 seconds over all four flow cells. Regeneration of the flow cells was done using a 10 second injection of 6 M guanidine-HCL. As a control for chip quality FlhD₄C₂ alone was always run at the beginning, middle and end of an experimental set. For protein-protein interactions standard BIAcore

protocols were followed using 300 RU of FliT immobilized on a CM5 sensor chip as ligand and either FliD or FliH₄C₂ as analyte.

Analytical Ultracentrifugation

Sedimentation velocity (SV) experiments were carried out in a ProteomeLab XL-I analytical ultracentrifuge (Beckman Coulter, USA) using both absorbance (at 280 nm) and interference optics. All AUC runs were carried out at a rotation speed of 48,000 rpm and an experimental temperature of 4°C using an 8-hole rotor and double-sector aluminium-epon centrepieces. The sample volume was 400 µl for the SV experiments with sample concentrations between 0.2 and 1.2 mg/ml. The partial specific volumes (\bar{v}) for the proteins were calculated from the protein amino acid sequence, using the program SEDNTERP and extrapolated to the experimental temperature. The density and viscosity of the buffer (10 mM Tris pH 7.5, 1 mM EDTA, 200 mM NaCl) at the experimental temperature was also calculated using SEDNTERP.

The distributions of sedimenting material were modelled as a distribution of Lamm equation solutions where the measured sedimentation boundary was modelled as an integral over differential concentration distributions $c(s)$ as implemented in the program SEDFIT (<http://www.analyticalultracentrifugation.com>) (Schuck, 1998). The sedimentation velocity profiles were fitted using a maximum entropy regularisation parameter of $p = 0.95$. The weight average sedimentation coefficient was calculated by integrating the differential sedimentation coefficient distribution (Schuck, 2003). Sedimentation coefficients (s) were extrapolated to zero concentration and converted to standard conditions, i.e. those that would be measured at 20°C in water. The diffusion coefficient (D) corresponding to each sedimentation coefficient value was estimated from a weight-average frictional ratio $(f/f_0)_w$

(Schuck, 1998; Schuck, 2003). Conversion to a molecular mass distribution from s and D was made using the Svedberg equation

$$M = \frac{sRT}{D(1 - \bar{v}\rho)},$$

where R is gas constant, T is temperature, \bar{v} is a partial specific volume of solute and ρ is density of the buffer. The integration of the mass distribution $c(M)$ was made similarly to the integration of $c(s)$ distribution in order to determine the weight average molecular mass of each species.

Acknowledgements

We would like to thank all lab members and colleagues for critical reading of this manuscript. Special thanks goes to W. Vollmer for his input. We would also like to thank R. Daniel, H. Murray and J. Errington for use of their microscope suite and M. Kinoshita-Minamino for technical assistance. Thanks also go to Bob Lightowlers for access and advice on the use of the BIAcore 2000. BBSRC Grant No. BB/D015855/1 awarded to P.A. funded the majority of this work. K.P was awarded a PhD scholarship from Naresuan University (Thailand). C.R. was partially supported by the National Science Foundation Grant CBET 0644744 and by Public Health Service Grants GM083601 and GM054365. Funding for K.I. and T.M is through the Targeted Proteins Research Program from the Ministry of Education, Science and Culture of Japan (K.I and T.M). An International Project Grant awarded jointly by the Diawa Foundation and Royal Society (UK) funded T.M. and P.A.

Table 1: Statistics of the FliM-GFP foci distribution in wild type. $\Delta fliT$ and $\Delta fliD$

Condition (YE g/L)	Strain	Growth rate - μ^*	Doubling time (min)*	Percentage of cells with FliM-GFP foci	Average number of FliM-GFP foci
0.04	Wild Type	0.0084	82.30	24	0.30 \pm 0.58
	$\Delta fliT$	0.0083	83.35	60	1.28 \pm 1.59
	$\Delta fliD$	0.0083	83.70	16	0.22 \pm 0.55
0.2	Wild Type	0.0089	77.52	38	0.50 \pm 0.81
	$\Delta fliT$	0.0089	77.57	62	2.88 \pm 3.88
	$\Delta fliD$	0.0088	79.02	26	0.30 \pm 0.54
1	Wild Type	0.0124	55.89	58	1.91 \pm 2.26
	$\Delta fliT$	0.0119	58.30	96	5.46 \pm 2.72
	$\Delta fliD$	0.0119	58.47	18	0.22 \pm 0.51
3	Wild Type	0.0138	50.16	90	3.74 \pm 2.41
	$\Delta fliT$	0.0135	51.30	92	5.32 \pm 3.27
	$\Delta fliD$	0.0133	52.01	54	1.40 \pm 1.74

*Calculated from 3 independent growth cultures. Standard deviations can be found in Table S1

Table 2: Strains and Plasmids used in this study

Strain No.	Strain/plasmid name	Genotype	Reference
	LT2	Wild type strain	K. Hughes
	BL21	$F^- ompT hsdSB dcm gal \lambda(DE3)$	Promega
	DH5 α	<i>phi-80d lac</i> Δ m15 <i>enda1 recA1 hsdR17 supE44 thh-1 gyrA96 relA ΔlacU169</i>	New England Biolabs
TPA14		$P_{flhDC}5451::Tn10[\text{del-25}]$	(Karlinsey <i>et al.</i> , 2000)
TPA20		<i>fliT::Km</i>	(Kutsukake <i>et al.</i> , 1999)
TPA993		Δ <i>fliT7046::tetRA</i>	
TPA1107	Wild type*	<i>fliM5978-gfp</i> (Mot+)	(Aldridge <i>et al.</i> , 2006a)
TPA2390	Δ <i>fliT</i> *	<i>fliM5978-gfp fliT::Km</i>	
TPA2421	Δ <i>fliD</i> *	<i>fliM5978-gfp ΔfliD7097::FRT</i>	
	pET28a-mod	His-tag plasmid	Novagen
	pGEX6p-1	GST expression plasmid	Stratagene
	pMMT002	<i>fliT94</i> in pGEX6p-1 (pGEX- <i>fliT</i> (2-94))	(Imada <i>et al.</i> , 2010)
	pMMT002(I68I)	<i>fliT94(I68A)</i> in pGEX6p-1	(Imada <i>et al.</i> , 2010)
	pMMT002(L72A)	<i>fliT94(L72A)</i> in pGEX6p-1	(Imada <i>et al.</i> , 2010)
	pMMT002(N74A)	<i>fliT94(N74A)</i> in pGEX6p-1	(Imada <i>et al.</i> , 2010)
	pMMT002(E75A)	<i>fliT94(E75A)</i> in pGEX6p-1	(Imada <i>et al.</i> , 2010)
	pMMT002(K79A)	<i>fliT94(K79A)</i> in pGEX6p-1	(Imada <i>et al.</i> , 2010)
	pMMT002(L81A)	<i>fliT94(L81A)</i> in pGEX6p-1	(Imada <i>et al.</i> , 2010)
	pMMT002(L82A)	<i>fliT94(L82A)</i> in pGEX6p-1	(Imada <i>et al.</i> , 2010)
	pMMT002(Q83A)	<i>fliT94(Q83A)</i> in pGEX6p-1	(Imada <i>et al.</i> , 2010)
	pPA152	<i>fliT</i> in pET28a-mod	
	pPA158	<i>flhDC</i> in pET28a-mod	
	pPA159	<i>fliD</i> in pET28a-mod	
	pRG38	P_{flhDC} in pSB401	(Goodier and Ahmer, 2001)
	pRG39:: <i>cat</i>	P_{fliC} in pSB401	(Brown <i>et al.</i> , 2008)
	pRG52:: <i>cat</i>	P_{flgB} in pSB401	(Brown <i>et al.</i> , 2008)
	pSE380		Invitrogen
	pSE- <i>fliT</i>	<i>fliT</i> in pSE380	
	pSE- <i>fliT94</i>	<i>fliT94</i> in pSE380	
	pSE- <i>flgM</i>	<i>flgM</i> in pSE380	
	pSE- <i>fliA</i>	<i>fliA</i> in pSE380	

* Names used in conjunction with Figure 1 and Table 1.

Table 3: DNA Sequences used for SPR analysis.

Name	Sequence [§]
P_{flgB}	CCCGTGTGAAGCAAGCATC AACGCAATAAATAGCG ACGCATTTT CGTTTATTCCGGCGATA AACGCGCGCGTGAAGGCAT
P_{flhB}	CGTATCCGGCTATCTCTATT AACGCCATAAACCCCG CCTTTTTTTAC CGCTTACTCTGCCTAT TGGCGTAAAGCGGTTCTG
$fliC$	TACGGGGGAACTGGTAAAGATGGCTATTATGAAGTTTCCGTTGATAAGACGAACGGTGAGGTGACTCTTGCTGGCGGTG

§ The FlhD₄C₂ inverted repeat as defined by Stafford *et al.*, (2005) is shown in bold.

For Peer Review

Figure Legends

Figure 1: Effect of growth conditions on the distribution of FliM-GFP foci in wild type (**A**), $\Delta fliT$ (**B**) and $\Delta fliD$ (**C**) strains. Growth conditions are described in the text and Materials and Methods. Black: MinE + 0.04 g/L YE; Gray: MinE + 0.2 g/L YE; Hashed: MinE + 1 g/L YE and White: MinE + 3 g/L YE. FliM-GFP foci were observed at 270 minutes after dilution, a time point defined as late log phase. The data shown is one data set of each strain grown at 30°C for 270 minutes where $n = 50$ cells for each strain in each condition were counted. The results have been confirmed by a minimum of 3 independent repeats.

Figure 2: Plasmid-based expression of FliT and FliT94 is unable to halt flagellar gene expression. (**A**) Motility assays of pSE380, pSE-*fliT*, pSE-*fliT94* and pGST-*fliT94* in comparison to pSE-*flgM* and pSE-*fliA* in LT2 after 8 hrs at 30°C. (**B**) Temporal gene expression assay comparing a vector control (triangles), pSE-*fliT* (circles) and pSE-*fliT94* (diamonds). The activities of the promoters P_{flgA} (P_{class2}) (black line, solid symbols) and P_{fliC} (P_{class3}) (grey lines, open symbols) are shown. Plasmid-based expression is able to delay activation of both promoter classes but activity and hierarchical expression is still observed. A stronger delay for P_{flgA} is observed for pSE-*fliT94*, consistent with the regulatory role of $\alpha 4$ to modulate FliT activity. For clarity the P_{fliC} activity for pSE-*fliT* and pSE-*fliT94* are plotted on the second Y-axis. This level of P_{fliC} activity is still sufficient to sustain a low level of motility as seen in (**A**). The data shown in (**B**) is an average of $n = 10$ repeats.

Figure 3: Analytical ultracentrifugation analysis of the interaction of FliT with FlhD₄C₂. In the buffer conditions used FliT alone (grey solid line) behaves as a dimer with a molecular

weight of 28 kDa while the FlhD₄C₂ complex (black solid line) was calculated to have a mass of 94.9 kDa in agreement with the published crystal structure (Wang *et al.*, 2006). Addition of FliT to FlhD₄C₂ in a 1:1 ratio (black short dashed line) significantly reduced the FlhD₄C₂ peak. Surprisingly no new species of greater mass was identified. Instead a shoulder to the left of the FlhD₄C₂ peak was observed. When using greater FliT:FlhD₄C₂ ratios at 5:1 (black long dashed line) or 10:1 (grey intermittent dashed line) this shoulder developed into an individual peak with a calculated mass of 61-63 kDa.

Figure 4: SPR analysis of FliT regulation of the FlhD₄C₂:DNA interaction. (A) Concentration dependent binding of FlhD₄C₂ to P_{flgB} (black lines, solid symbols) and the inhibition of the interaction with 1:1 molar ratios of FliT (grey lines, open symbols). Circles: 200 nM; squares: 100 nM and triangles: 50 nM. A buffer control (diamonds) is also included. (B) Analysis of the amount of FliT required to inhibit FlhD₄C₂:P_{flgB} DNA complex formation. All assays were performed using 100 nM FlhD₄C₂. Circles: No FliT; squares: 100 nM FliT; triangles: 150 nM FliT; diamonds: 250 nM FliT; inverted triangles: 400 nM FliT. A buffer control (grey line) is also included. No further change was observed for concentrations higher than 400 nM FliT (data not shown).

Figure 5: A FlhD₄C₂:DNA complex is insensitive to FliT. (A) SPR profile of injection of buffer (grey dashes) or 100 nM FliT (black) over FlhD₄C₂:P_{flgB} DNA complex. A similar result with the other DNA species and higher FliT concentrations was observed (data not shown). The arrows indicate the injection start time and stop time. The binding of FlhD₄C₂ to the DNA is not shown for clarity. (B) Unlabelled P_{flgB} DNA is able to compete for bound FlhD₄C₂. SPR profiles showing the effect of injecting 100 nM P_{flgB} unlabelled DNA over FlhD₄C₂ bound to P_{flgB} (solid line), P_{flhB} (short dashed line) and an intergenic region of *fliC* (long dashes).

Figure 6: FliD acts as an anti-anti-FlhD₄C₂ factor. SPR profiles of the influence of FliD on the ability of FliT to inhibit the FlhD₄C₂:P_{fliB} DNA interaction. In all experiments a 1:1 ratio of all components was used using a concentration of 100 nM. Circles: FlhD₄C₂ alone; triangles: FlhD₄C₂ + FliT; inverted triangles: FlhD₄C₂ + FliD; squares: FlhD₄C₂ + FliT + FliD and Gray Diamonds: Buffer control. Here resonance units are expressed relative to the maximal RU of FlhD₄C₂ alone.

Figure 7: Autoregulation of P_{class1} (P_{fliDC}) by FlhD₄C₂ responds to FliT inhibition of FlhD₄C₂. P_{fliDC} activity was monitored over time in a growing culture. The change in P_{fliDC} activity in the Δ fliT mutant compared to wild type was used in the genetic screen for fliT mutations. Wild type: circles; Δ fliT: diamonds; Δ fliD: squares; and Δ fliDC: triangles. Deletion of Δ fliD did not show such a strong change in P_{fliDC} activity, as did deletion of fliT or fliDC. Activity was calculated relative to optical density as described in Materials and Methods.

Figure 8: The interaction interface of FliT for FliD and FlhD₄C₂ overlap. **(A)** Motility assays using semi-solid agar of SJW1103 expressing *gst-fliT94* with a series of alanine substitutions in α 3 of FliT from the plasmid pGEX6p-1. **(B)** Immunoblot analysis using polyclonal anti-FlhC antibody of a GST-pull down assay of GST-FliT94 and its variants when expressed in *S. enterica*. The efficiency of isolating FlhC using E75A is significantly reduced (Imada *et al.*, 2010). **(C)** SPR analysis of *fliT94* compared to alleles containing N74A, E75A, K79A and L82A amino acid substitutions. FlhD₄C₂ alone and FlhD₄C₂ with FliT94 are shown as black lines in each data set for comparison. Each mutant is shown as short dashed grey lines. Circles: 100 nM FlhD₄C₂: 100 nM FliT94; diamonds: 100 nM FlhD₄C₂ : 200 nM FliT94; triangles: 100 nM FlhD₄C₂: 400 nM FliT94; squares: buffer

control, the same symbols are used for the same molar ratios of the alanine substitutions tested. Consistent with the motility data in **(A)**, E75A showed the weakest ability to inhibit FlhD₄C₂ to interact with P_{flgB} DNA.

For Peer Review

References

- Adler, J. and Templeton B. (1967) The effect of environmental conditions on the motility of *Escherichia coli*. *J Gen Microbiol* **46**: 175-184.
- Aldridge, P., Karlinsey J. and Hughes K. T. (2003) The type III secretion chaperone FlgN regulates flagellar assembly via a negative feedback loop containing its chaperone substrates FlgK and FlgL. *Mol Microbiol* **49**: 1333-1345.
- Aldridge, P., Karlinsey J. E., Becker E., Chevance F. F. and Hughes K. T. (2006a) Flk prevents premature secretion of the anti-sigma factor FlgM into the periplasm. *Mol Microbiol* **60**: 630-643.
- Aldridge, P. D., Karlinsey J. E., Aldridge C., Birchall C., Thompson D., Yagasaki J. and Hughes K. T. (2006b) The flagellar-specific transcription factor, σ^{28} , is the Type III secretion chaperone for the flagellar-specific anti- σ^{28} factor FlgM. *Genes Dev* **20**: 2315-2326.
- Bange, G., Kummerer N., Engel C., Bozkurt G., Wild K. and Sinning I. (2010) FlhA provides the adaptor for coordinated delivery of late flagella building blocks to the type III secretion system. *Proc Natl Acad Sci U S A* **107**: 11295-11300.
- Barkai, N. and Leibler S. (1997) Robustness in simple biochemical networks. *Nature* **387**: 913-917.
- Bonifield, H. R., Yamaguchi S. and Hughes K. T. (2000) The flagellar hook protein, FlgE, of *Salmonella enterica* serovar Typhimurium is posttranscriptionally regulated in response to the stage of flagellar assembly. *J Bacteriol* **182**: 4044-4050.
- Brown, J. D., Saini S., Aldridge C., Herbert J., Rao C. V. and Aldridge P. D. (2008) The rate of protein secretion dictates the temporal dynamics of flagellar gene expression. *Mol Microbiol* **70**: 924-937.

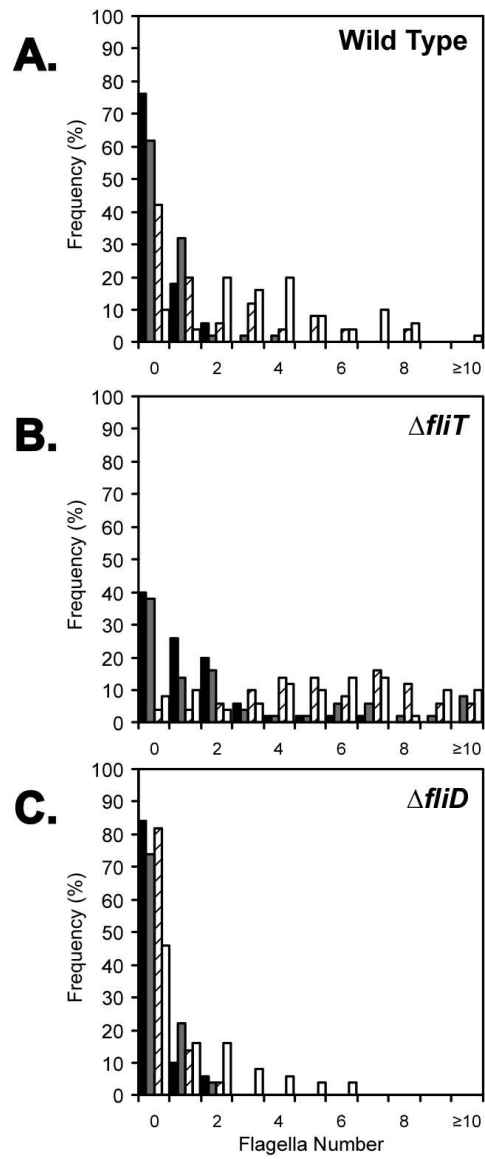
- Chilcott, G. S. and Hughes K. T. (2000) Coupling of Flagellar Gene Expression to Flagellar Assembly in *Salmonella enterica* Serovar Typhimurium and *Escherichia coli*. *Microbiol Mol Biol Rev.*
- Claret, L. and Hughes C. (2000) Functions of the subunits in the FlhD(2)C(2) transcriptional master regulator of bacterial flagellum biogenesis and swarming. *J Mol Biol* **303**: 467-478.
- Darnton, N., Turner L., Rojevsky S. and Berg H. C. (2007) On torque and tumbling in swimming *Escherichia coli*. *J Bacteriol* **189**: 1756-1764.
- Datsenko, K. A. and Wanner B. L. (2000) One-step inactivation of chromosomal genes in *Escherichia coli* K-12 using PCR products. *Proc Natl Acad Sci U S A* **97**: 6640-6645.
- Davis, R. W., Botstein D., Roth J. R. and Cold Spring Harbor N.Y. Laboratory of Quantitative Biology (1980) *Advanced bacterial genetics: a manual for genetic engineering*. Cold Spring Harbor Laboratory, Cold Spring Harbor, N.Y.
- Erhardt, M. and Hughes K. T. (2010) C-ring requirement in flagellar type III secretion is bypassed by FlhDC upregulation. *Mol Microbiol* **75**: 376-393.
- Evans, L. D., Stafford G. P., Ahmed S., Fraser G. M. and Hughes C. (2006) An escort mechanism for cycling of export chaperones during flagellum assembly. *Proc Natl Acad Sci U S A* **103**: 17474-17479.
- Fraser, G. M., Bennett J. C. and Hughes C. (1999) Substrate-specific binding of hook-associated proteins by FlgN and FliT, putative chaperones for flagellum assembly. *Mol Microbiol* **32**: 569-580.
- Gillen, K. L. and Hughes K. T. (1991a) Molecular characterization of *flgM*, a gene encoding a negative regulator of flagellin synthesis in *Salmonella typhimurium*. *J Bacteriol* **173**: 6453-6459.

- Gillen, K. L. and Hughes K. T. (1991b) Negative regulatory loci coupling flagellin synthesis to flagellar assembly in *Salmonella typhimurium*. *J Bacteriol* **173**: 2301-2310.
- Goodier, R. I. and Ahmer B. M. (2001) SirA orthologs affect both motility and virulence. *J Bacteriol* **183**: 2249-2258.
- Hughes, K. T., Gillen K. L., Semon M. J. and Karlinsey J. E. (1993) Sensing structural intermediates in bacterial flagellar assembly by export of a negative regulator. *Science* **262**: 1277-1280.
- Iino, T. (1974) Assembly of *Salmonella* flagellin *in vitro* and *in vivo*. *J Supramol Struct* **2**: 372-384.
- Imada, K., Minamino T., Kinoshita M., Furukawa Y. and Namba K. (2010) Structural insight into the regulatory mechanisms of interactions of the flagellar type III chaperone FliT with its binding partners. *Proc Natl Acad Sci U S A*.
- Karlinsey, J. E., Tanaka S., Bettenworth V., Yamaguchi S., Boos W., Aizawa S. I. and Hughes K. T. (2000) Completion of the hook-basal body complex of the *Salmonella typhimurium* flagellum is coupled to FlgM secretion and *fliC* transcription. *Mol Microbiol* **37**: 1220-1231.
- Kutsukake, K. and Iino T. (1994) Role of the FliA-FlgM regulatory system on the transcriptional control of the flagellar regulon and flagellar formation in *Salmonella typhimurium*. *J Bacteriol* **176**: 3598-3605.
- Kutsukake, K., Ikebe T. and Yamamoto S. (1999) Two novel regulatory genes, *fliT* and *fliZ*, in the flagellar regulon of *Salmonella*. *Genes Genet Syst* **74**: 287-292.
- Liu, X., Fujita N., Ishihama A. and Matsumura P. (1995) The C-terminal region of the alpha subunit of *Escherichia coli* RNA polymerase is required for transcriptional activation of the flagellar level II operons by the FlhD/FlhC complex. *J Bacteriol* **177**: 5186-5188.

- Murray, H. and Errington J. (2008) Dynamic control of the DNA replication initiation protein DnaA by Soj/ParA. *Cell* **135**: 74-84.
- Ohnishi, K., Kutsukake K., Suzuki H. and Iino T. (1990) Gene *fliA* encodes an alternative sigma factor specific for flagellar operons in *Salmonella typhimurium*. *Mol Gen Genet* **221**: 139-147.
- Overgaard, M., Borch J., Jorgensen M. G. and Gerdes K. (2008) Messenger RNA interferase RelE controls *relBE* transcription by conditional cooperativity. *Mol Microbiol* **69**: 841-857.
- Pruss, B. M. and Matsumura P. (1996) A regulator of the flagellar regulon of *Escherichia coli*, *flhD*, also affects cell division. *J Bacteriol* **178**: 668-674.
- Pruss, B. M. and Matsumura P. (1997) Cell cycle regulation of flagellar genes. *J Bacteriol* **179**: 5602-5604.
- Saijo-Hamano, Y., Imada K., Minamino T., Kihara M., Shimada M., Kitao A. and Namba K. (2010) Structure of the cytoplasmic domain of FlhA and implication for flagellar type III protein export. *Mol Microbiol* **76**: 260-268.
- Saini, S., Brown J. D., Aldridge P. D. and Rao C. V. (2008) FlhZ is a posttranslational activator of FlhD₄C₂-dependent flagellar gene expression. *J Bacteriol* **190**: 4979-4988.
- Schaechter, M., Maaloe O. and Kjeldgaard N. O. (1958) Dependency on medium and temperature of cell size and chemical composition during balanced growth of *Salmonella typhimurium*. *J Gen Microbiol* **19**: 592-606.
- Schuck, P. (1998) Sedimentation analysis of noninteracting and self-associating solutes using numerical solutions to the Lamm equation. *Biophys J* **75**: 1503-1512.
- Schuck, P. (2003) On the analysis of protein self-association by sedimentation velocity analytical ultracentrifugation. *Anal Biochem* **320**: 104-124.

- Soutourina, O. A. and Bertin P. N. (2003) Regulation cascade of flagellar expression in Gram-negative bacteria. *FEMS Microbiol Rev* **27**: 505-523.
- Stafford, G. P., Ogi T. and Hughes C. (2005) Binding and transcriptional activation of non-flagellar genes by the *Escherichia coli* flagellar master regulator FlhD₂C₂. *Microbiology* **151**: 1779-1788.
- Turner, L., Ryu W. S. and Berg H. C. (2000) Real-time imaging of fluorescent flagellar filaments. *J Bacteriol* **182**: 2793-2801.
- Vogel, H. J. and Bonner D. M. (1956) Acetylornithinase of *Escherichia coli*: partial purification and some properties. *J Biol Chem* **218**: 97-106.
- Wang, S., Fleming R. T., Westbrook E. M., Matsumura P. and McKay D. B. (2006) Structure of the *Escherichia coli* FlhDC complex, a prokaryotic heteromeric regulator of transcription. *J Mol Biol* **355**: 798-808.
- Yamamoto, S. and Kutsukake K. (2006) FlIT acts as an anti-FlhD₂C₂ factor in the transcriptional control of the flagellar regulon in *Salmonella enterica* serovar Typhimurium. *J Bacteriol* **188**: 6703-6708.

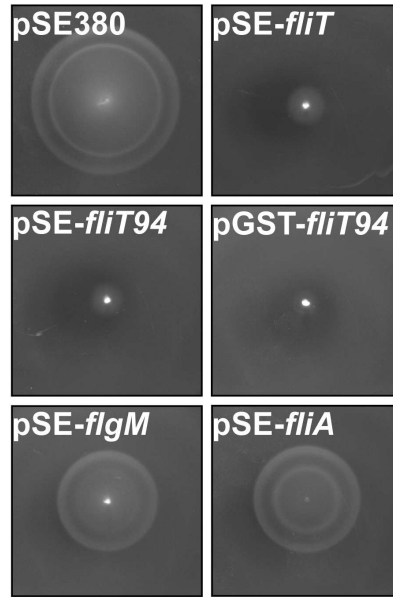
Figure 1



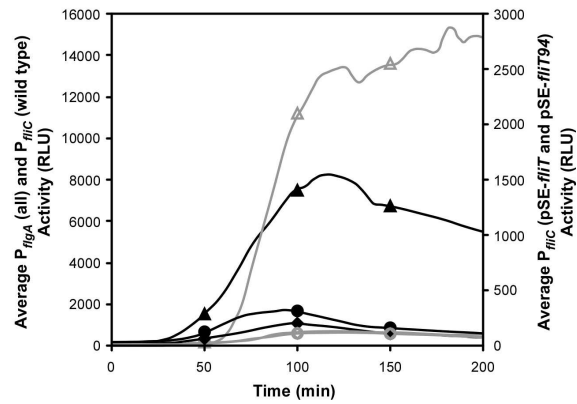
128x274mm (150 x 150 DPI)

Figure 2

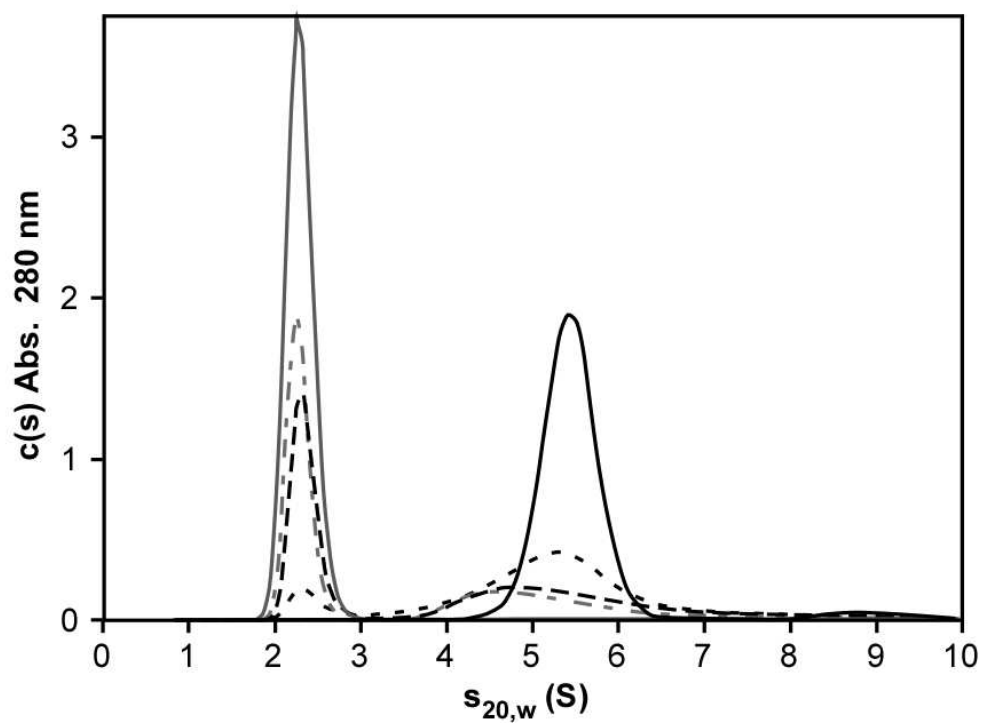
A.



B.



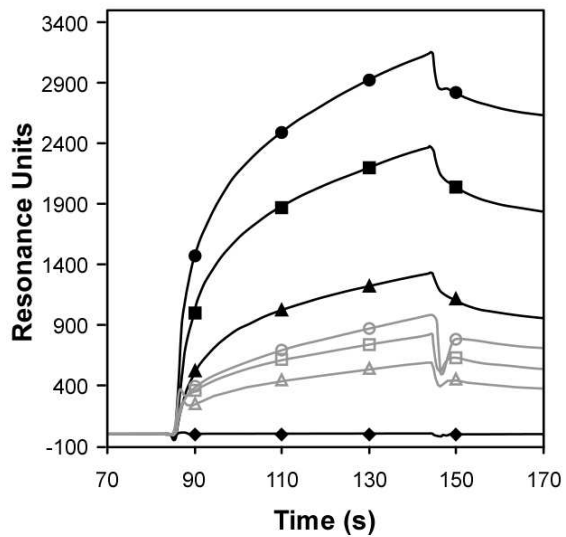
130x230mm (300 x 300 DPI)

Figure 3

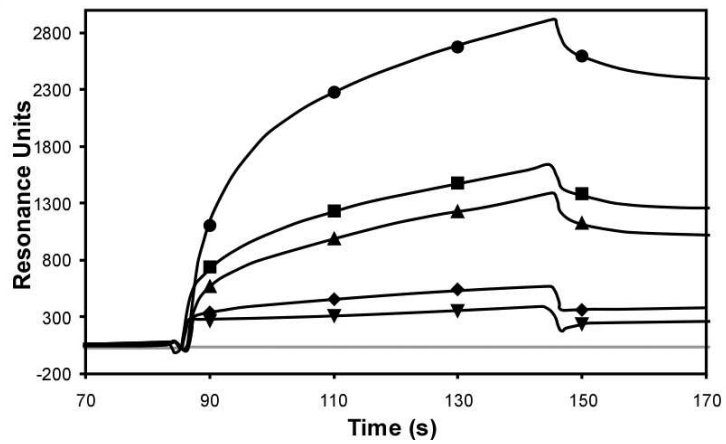
147x123mm (150 x 150 DPI)

Figure 4

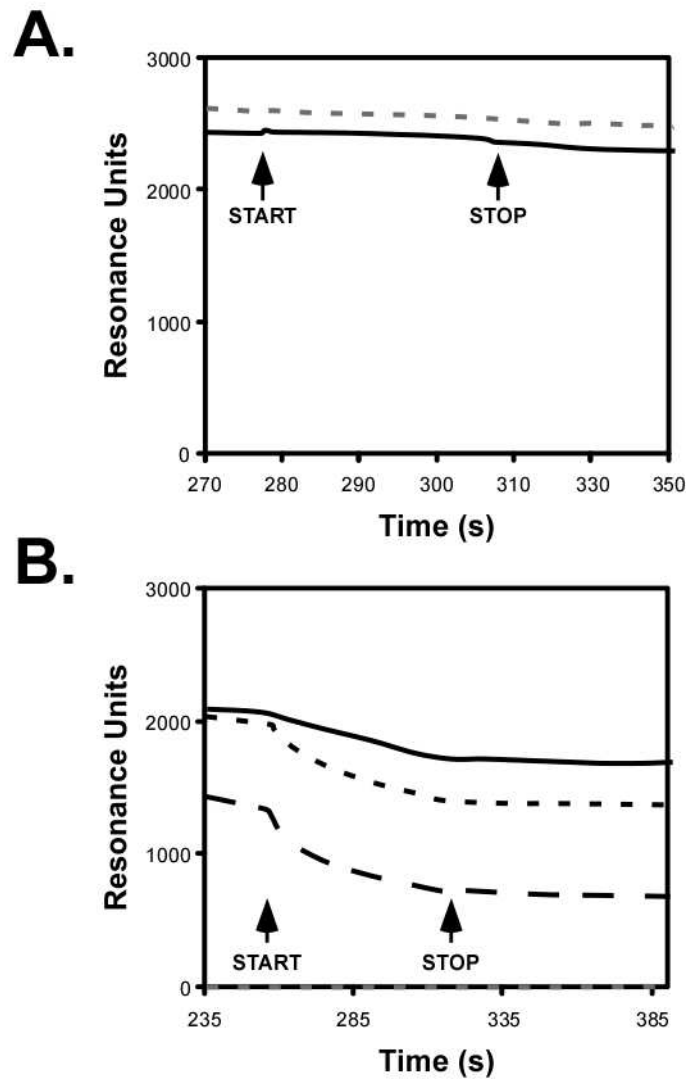
A.



B.

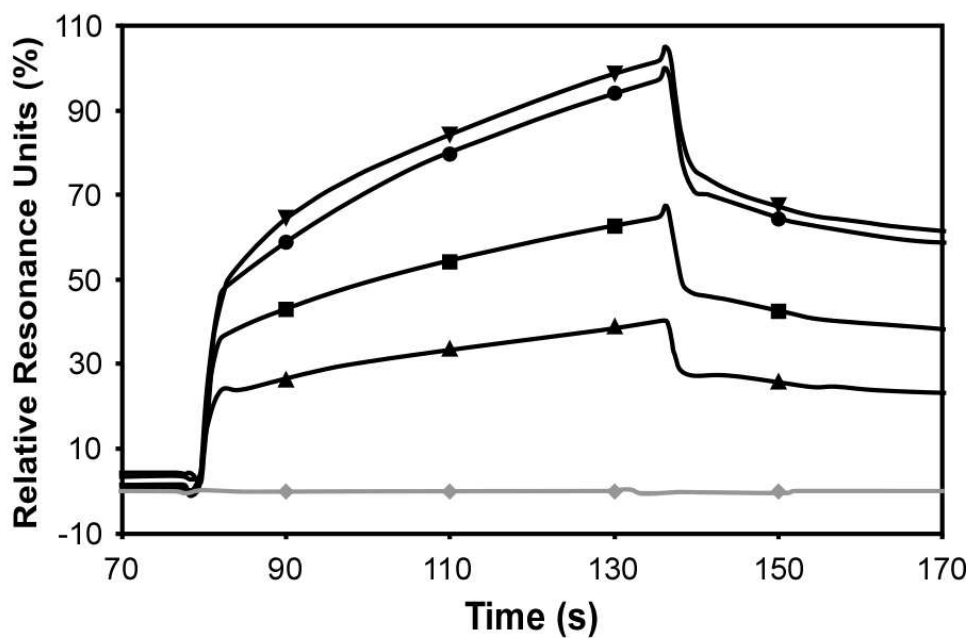


143x224mm (150 x 150 DPI)

Figure 5

107x158mm (150 x 150 DPI)

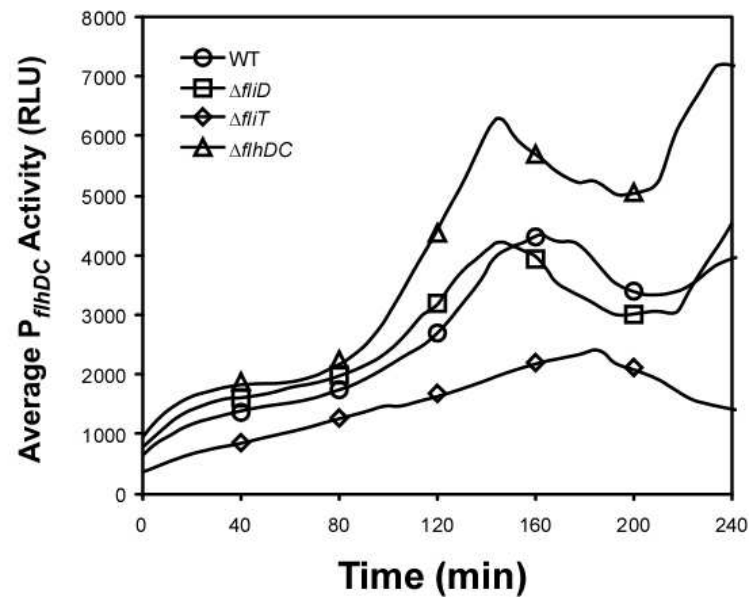
Figure 6



159x123mm (150 x 150 DPI)

Review

Figure 7



125x93mm (150 x 150 DPI)

review

Figure 8

